JOURNAL OF VIROLOGY, June 2010, p. 5485–5493 Vol. 84, No. 11
0022-538X/10/$12.00 doi:10.1128/JVI.02250-09


# Japanese Encephalitis Virus Utilizes the Canonical Pathway To Activate NF-κB but It Utilizes the Type I Interferon Pathway To Induce Major Histocompatibility Complex Class I Expression in Mouse Embryonic Fibroblasts▽†

Sojan Abraham,[1]‡ Ashwini Sankrepatna Nagaraj,[1]§ Soumen Basak,[2]‖ and Ramanathapuram Manjunath[1]*

*Department of Biochemistry, Indian Institute of Science, Bangalore 560 012, India,[1] and Signaling Systems Laboratory and Department of Chemistry and Biochemistry, University of California, San Diego, 9500 Gilman Dr., La Jolla, California 92093-0375[2]*

Received 24 October 2009/Accepted 18 March 2010

**Flaviviruses have been shown to induce cell surface expression of major histocompatibility complex class I (MHC-I) through the activation of NF-κB. Using IKK1$^{-/-}$, IKK2$^{-/-}$, NEMO$^{-/-}$, and IKK1$^{-/-}$ IKK2$^{-/-}$ double mutant as well as p50$^{-/-}$ RelA$^{-/-}$ cRel$^{-/-}$ triple mutant mouse embryonic fibroblasts infected with Japanese encephalitis virus (JEV), we show that this flavivirus utilizes the canonical pathway to activate NF-κB in an IKK2- and NEMO-, but not IKK1-, dependent manner. NF-κB DNA binding activity induced upon virus infection was shown to be composed of RelA:p50 dimers in these fibroblasts. Type I interferon (IFN) production was significantly decreased but not completely abolished upon virus infection in cells defective in NF-κB activation. In contrast, induction of classical MHC-I (class 1a) genes and their cell surface expression remained unaffected in these NF-κB-defective cells. However, MHC-I induction was impaired in IFNAR$^{-/-}$ cells that lack the alpha/beta IFN receptor, indicating a dominant role of type I IFNs but not NF-κB for the induction of MHC-I molecules by Japanese encephalitis virus. Our further analysis revealed that the residual type I IFN signaling in NF-κB-deficient cells is sufficient to drive MHC-I gene expression upon virus infection in mouse embryonic fibroblasts. However, NF-κB could indirectly regulate MHC-I expression, since JEV-induced type I IFN expression was found to be critically dependent on it.**

*Japanese encephalitis virus* (JEV) is a positive-stranded RNA virus that belongs to the *Flavivirus* genus of the family *Flaviviridae* (28). The epidemiological, pathological, immunological, and structural aspects of this neurotropic virus have been well studied (15, 16, 23, 37). Flaviviruses have been shown to upregulate the cell surface expression of major histocompatibility complex (MHC) molecules as well as molecules associated with antigen presentation and cell adhesion (8, 9, 23). We have reported that JEV infection induces the expression of nonclassical MHC class I (MHC-I) molecules in addition to classical MHC-I (2). Many of these flavivirus-mediated effects on MHC-I and cell adhesion molecules have been shown to be due to the activation of the ubiquitous transcriptional factor nuclear factor κB (NF-κB) (22).

The NF-κB family of transcription factors consists of more than a dozen homo- or heterodimers composed of five Rel proteins, namely, RelA, RelB, cRel, p50, and p52. In the resting cell, NF-κB dimers are retained in the cytoplasm in an inactive state by three inhibitor proteins, IκBα, IκBβ, and IκBε. In the canonical pathway, stimulus-responsive phosphorylation of the IκBs by IκB kinase (IKK) complex leads to their degradation to allow for nuclear translocation of the NF-κB dimers, mostly RelA:p50 dimers. The IKK complex is composed of two catalytic subunits, IKK1 (IKKα) and IKK2 (IKKβ), as well as a regulatory subunit, NEMO. IKK1 kinase activity was shown to be dispensable for the NF-κB activation through the canonical pathway (13, 25, 35). However, stimuli that utilize the noncanonical pathway critically depend on the IKK1 activity to induce NF-κB dimers. In the noncanonical pathway, IKK1-mediated phosphorylation of the NF-κB precursor protein p100 leads to its proteasomal processing into the mature p52 subunit, which then dimerizes with RelB to appear as the nuclear RelB:p52 dimer (3, 36, 39).

Modulation of the NF-κB and type I interferon (IFN) pathways during immune responses and viral infections is well characterized (14, 17, 19, 32). West Nile virus (WNV), also a flavivirus, has been shown to induce both MHC-II and MHC-I molecules. MHC-I was induced by NF-κB-dependent as well as NF-κB-independent pathways. The former was type I IFN independent, while the latter was type I IFN dependent (8). However, JEV has been shown to induce MHC-I but is unable to induce MHC-II (1). Given distinct regulations of the canonical and the noncanonical pathways, it was of interest to delineate the mechanism underlying NF-κB activation in response

* Corresponding author. Mailing address: Department of Biochemistry, Indian Institute of Science, Bangalore 560 012, India. Phone: 91-80-22932309. Fax: 91-80-23600814. E-mail: mjnhm@biochem.iisc.ernet.in.

† Supplemental material for this article may be found at http://jvi.asm.org/.

‡ Present address: Department of Biomedical Sciences, Center of Excellence for Infectious Diseases, Paul L. Foster School of Medicine, Texas Tech University Health Sciences Center, 5001 El Paso Drive, El Paso, TX 79905.

§ Present address: Syngene International Ltd., Biocon Park, Plot 243, Bommasandra Industrial Estate, Phase IV, Bommasandra-Jigani Link Road, Bangalore 560 099, India.

‖ Present address: National Institute of Immunology, Aruna Asaf Ali Marg, New Delhi 110 067, India.

▽ Published ahead of print on 31 March 2010.

to JEV infection and to evaluate the role of the NF-κB pathway in MHC-I gene expression.

Using mutant and wild-type (WT) mouse embryonic fibroblasts (MEFs), we show here for the first time that JEV utilizes the canonical pathway of NF-κB activation that is dependent on both IKK2 and NEMO subunits of the IKK complex. Our results show that JEV-induced production of type I IFNs is reduced in cells deficient in NF-κB signaling and point to an important role for the NF-κB/RelA:p50 dimer in the induction of type I IFNs during JEV infection. However, we also show that type I IFNs, not NF-κB, are predominantly responsible for the induction of classical MHC-I molecules during JEV infection and that residual IFNs produced via NF-κB-independent mechanisms are sufficient for MHC-I gene expression in NF-κB-deficient cells.

## MATERIALS AND METHODS

**Media, antibodies, and cell lines.** Dulbecco's modified Eagle's medium (DMEM), fetal calf serum (FCS), poly(dI-dC), and Trizol were purchased from Sigma-Aldrich India. Polynucleotide kinase and Revert Aid Moloney murine leukemia virus (M-MuLV) reverse transcriptase were obtained from MBI Fermentas, Lithuania. Anti-H-2K$^b$D$^b$ (clone 28-8-6) monoclonal antibody (MAb) was obtained from BD Pharmingen, while goat anti-mouse IgG (Fcγ chain specific) was from Jackson Immunoresearch Labs. A flavivirus group-specific MAb (clone DI-4G2-4-15) was used as a hybridoma supernatant. Antibodies specific to p50 and p65 subunits of the NF-κB complex were obtained from Santa Cruz Biotechnology. Alpha interferon (IFN-α) and IFN-β detection enzyme-linked immunosorbent assay (ELISA) kits were obtained from PBL Biomedical Laboratories.

Wild-type (H-2K$^b$D$^b$), IKK1$^{-/-}$, IKK2$^{-/-}$, and IKK1$^{-/-}$ IKK2$^{-/-}$ MEFs were provided by Inder Verma (Salk Institute of Biological Science, La Jolla, CA); NEMO$^{-/-}$ MEFs were provided by Marc Schmidt Supprian (Harvard Medical School, Boston, MA). Reconstituted MEFs and p50$^{-/-}$ RelA$^{-/-}$ cRel$^{-/-}$ MEFs were provided by Alexander Hoffmann (University of California, San Diego, CA). IFNAR$^{-/-}$ MEFs were provided by Otto Haller, University of Freiburg, Germany. All the cells were grown in DMEM supplemented with 10% FCS and antibiotics. The ability of the wild-type (WT) and all mutant MEFs to respond either to tumor necrosis factor alpha (TNF-α) treatment (which activates the canonical NF-κB pathway) or to lymphotoxin beta receptor (LTβR) agonistic antibody treatment (which activates the noncanonical NF-κB pathway) was first verified by functional assays before the MEFs were used in the study (see Fig. S1 in the supplemental material). IFNAR-knockout MEFs that lack the alpha/beta IFN receptor were verified by their inability to induce cell surface expression of MHC-I upon type I IFN treatment. H6 (A/J mouse-derived hepatoma H-2K$^k$D$^d$) cells were grown in RPMI 1640 supplemented with 10% FCS. PS (porcine kidney) cells were grown in minimum essential medium (MEM) supplemented with 10% FCS and used for virus titrations, while C6/36 mosquito cells were grown in MEM supplemented with 10% FCS and 10% tryptose phosphate broth and used for virus collection.

**Virus collection, titration, and infection of cells.** JEV strain P20778, an isolate from human brain, was used to infect C6/36 mosquito cells that were grown to confluence at 28°C. Cells were infected at a multiplicity of infection (MOI) of 1 for 2 h at 28°C and maintained in MEM containing 2.5% FCS. Cell supernatants were collected every 8 h for a period of 80 h and stored at −70°C before being used for infection of cell lines. Virus titers were determined by PFU assays on PS cells (1).

For infection, all the cells, including wild-type and mutant MEFs, were adsorbed with virus at an MOI of 1 for 2 h, washed once, and cultured in fresh medium containing 2.5% FCS. The cells were harvested after different times postinfection (p.i.) and used for RNA and nuclear extract preparation as well as fluorescence-activated cell sorting (FACS) analysis. Control cells were incubated with fluid collected from uninfected C6/36 cells.

**Semiquantitative reverse transcription-PCR (RT-PCR) analysis.** Total RNA was isolated from infected and control cells using Trizol reagent according to the manufacturer's instructions. The sequence of the gene-specific primers used in this study and the procedure for PCR analysis have been previously published (2). Briefly, 1.5 μg of total RNA was used for reverse transcription using Revert Aid M-MuLV reverse transcriptase. The oligo(dT)-primed cDNA was diluted 100×, 4 μl of the diluted cDNA was used for PCRs using gene-specific primers, and the products were resolved on 1.5% agarose gels. Several standardization experiments were performed to ensure the semiquantitative nature of the results obtained.

**Quantitative real-time RT-PCR analysis.** The real-time RT-PCR for the quantification of MHC-I, IFN-β, and IFN-α mRNA was performed with the Express SYBR GreenER qPCR Supermix (Invitrogen). PCR amplification was performed in an Applied Biosystems 7900 HT fast real-time PCR system (Applied Biosystems, Foster City, CA). Real-time PCR mixtures contained 5 μl of 2× SYBR green Supermix, 1 μl of each primer, and 1.0 μl template cDNA, and water was added to a final volume of 10 μl. Samples were subjected to the following thermal cycling conditions: 50°C for 2 min and 95°C for 2 min, followed by 40 cycles of 95°C for 15 s and 60°C for 1 min. The final stage consisted of 95°C for 15 s, 60°C for 15 s, and 95°C for 15 s. This additional step allowed us to check the melting temperature of the formed amplicons and thus the specificity of the primers. For data analysis, the threshold cycle ($2^{-\Delta\Delta Ct}$) method was used to calculate fold change and glyceraldehyde-3-phosphate dehydrogenase (GAPDH) expression was used as a reference gene for normalization of threshold cycles (Ct). The specific primers used were as follows: K$^b$, 5′-GCCCTCAGTTCTCTT TAGTCA-3′ and 5′-GCCCTAGGTCAAGATGATAAC-3′; D$^b$, 5′-CCCTGAA CGAAGACCTGAAAACG-3′ and 5′-CAGCAACGATCACCATGTAAGAG TCAG-3′; IFN-α, 5′-CCTCCTAGACTCATTCTGCAAT-3′ and 5′-CACAGG GGCTGTGTTTCTTC-3′; IFN-β, 5′-AAGAGTTACACTGCCTTTGCCAT C-3′ and 5′-CACTGTCTGCTGGTGGAGTTCATC-3′; GAPDH, 5′-AGGTCG GTGTGAACGGATTTGGC-3′ and 5′-CTAAGCAGTTGGTGGTGGTGCAG GATGC-3′.

**Flow cytometric analysis (FACS).** Cells ($0.5 \times 10^6$) were harvested and incubated with the primary antibody at 4°C for 1 h. After incubation, the cells were washed once with wash medium (DMEM with 1% FCS) and then incubated with the secondary antibody at 4°C for 1 h. After being washed with wash medium, the cells were fixed with 1.5% paraformaldehyde. For intracellular staining, cells were fixed with BD Cytofix/Cytoperm solution and stained as published (2). All samples were acquired using a FACScan cytometer (Becton Dickinson). Data analysis of 10,000 events acquired for each sample was done using WinList software.

**ELISA.** ELISA was carried out according to the manufacturer's instructions. Briefly, interferon standard samples and unknown samples were added along with appropriate controls to an antibody-precoated microtiter plate in duplicate. The plate was incubated for 1 h, washed with wash solution, and incubated with detection antibody solution for 24 h in the case of IFN-α ELISA and 4 h for IFN-β ELISA. Plates were washed three times, and horseradish peroxidase (HRP) conjugate solution was added for 1 h. After washing, tetramethylbenzidine (TMB) substrate solution was added and the reaction was stopped after 1 h. The absorbance was measured at 450 nm within 5 min after the addition of stop solution, and the concentration of IFN was determined. All incubations were carried out at 24°C.

**EMSA.** Cells ($3 \times 10^6$) were washed with phosphate-buffered saline (PBS) and resuspended in 400 μl ice-cold buffer A (10 mM HEPES, pH 7.9, 10 mM KCl, 0.1 mM EDTA, 0.1 mM EGTA, 1 mM dithiothreitol [DTT], 0.5 mM phenylmethylsulfonyl fluoride [PMSF]) by gentle pipetting. The cells were allowed to swell on ice for 30 min, after which NP-40 was added to a final concentration of 0.6% and the suspension was vigorously vortexed. The suspension was centrifuged at 4°C for 2 min at 12,000 rpm, and the nuclear pellet was resuspended in 50 μl ice-cold buffer B (20 mM HEPES, pH 7.9, 0.4 M NaCl, 10 mM KCl, 1 mM EDTA, 1 mM EGTA, 1 mM DTT, and 1 mM PMSF) containing leupeptin and aprotinin (10 μg/ml). The tubes were vigorously rocked at 4°C for 30 min and centrifuged for 15 min in a microcentrifuge. The supernatants containing the nuclear proteins were stored at −70°C until analysis by Bradford assay and electrophoretic mobility shift assay (EMSA).

Double-stranded oligonucleotides containing the NF-κB consensus sequence (5′-AGTTGAGGGGACTTTCCCAGGC-3′) and mutant sequence (5′-AGTTG AGGCGACTTTCCCAGGC-3) were used for EMSA (31, 41). The oligonucleotides were end labeled with [γ-$^{32}$P]ATP using T4 polynucleotide kinase. EMSA was performed in a total volume of 20 μl at 4°C. Thirty micrograms of nuclear extracts was equilibrated for 20 min in binding buffer (10 mM Tris-HCl, pH 8.0, 75 mM KCl, 2.5 mM $MgCl_2$, 0.1 mM EDTA, 10% glycerol, 0.25 mM DTT) and 1 μg of poly(dI-dC). The mixture was incubated with $^{32}$P-labeled oligonucleotide probe for 30 min on ice. Protein-DNA complexes were separated by electrophoresis on 5% native polyacrylamide gels followed by autoradiography for visualization in a BioImage analyzer (FLA5100; Fuji Film, Japan).

For supershift assays, analysis was carried out with 2 μg of antibodies to p50 and p65 (RelA) subunits of the NF-κB complex by adding them individually before the labeled oligonucleotide to the binding reaction mixture and incubating them for 30 min at 4°C.

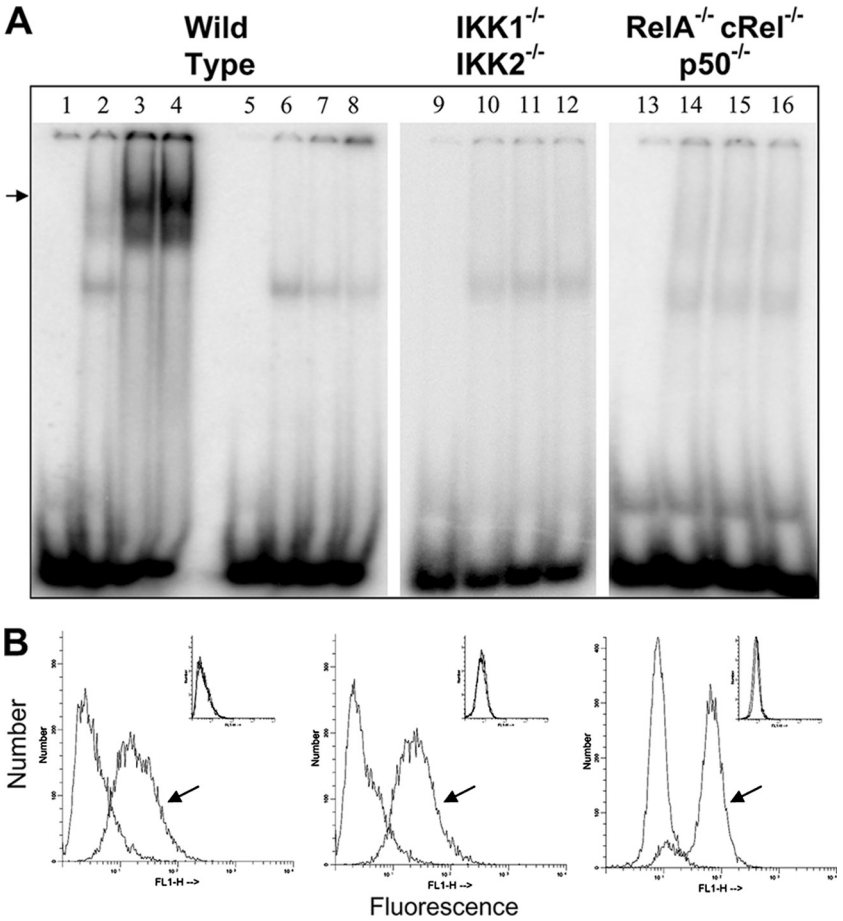


FIG. 1. Nuclear translocation of NF-κB in JEV-infected MEFs. (A) EMSA was performed using uninfected and JEV-infected wild-type, IKK1$^{-/-}$ IKK2$^{-/-}$, and RelA$^{-/-}$ cRel$^{-/-}$ p50$^{-/-}$ MEFs as indicated on top. Lanes 1 to 4 represent EMSA performed with NF-κB-specific oligomer, while lanes 5 to 8 represent EMSA performed with NF-κB mutant oligomer. Lanes 1, 5, 9, and 13 represent the oligomer alone; lanes 2, 6, 10, and 14 represent uninfected MEFs; and lanes 3, 7, 11, and 15 represent cells at 10 h p.i., while lanes 4, 8, 12, and 16 represent cells that were infected for 14 h. The arrow indicates the specific NF-κB–DNA complex. (B) As labeled in panel A, wild-type, IKK1$^{-/-}$ IKK2$^{-/-}$, and RelA$^{-/-}$ cRel$^{-/-}$ p50$^{-/-}$ MEFs that were infected with JEV for 12 h were stained for the expression of intracellular JEV antigen. The arrow indicates staining with primary antiflavivirus group-specific MAb followed by fluorescein isothiocyanate (FITC) anti-mouse secondary antibody, while the unmarked histogram indicates staining with secondary antibody alone. The two histograms overlap in the insets, which represent staining of uninfected cells.

## RESULTS

**JEV infection induces NF-κB DNA binding activity in wild-type but not in IKK1$^{-/-}$ IKK2$^{-/-}$ MEFs.** JEV infection was shown to induce nuclear translocation of the NF-κB dimers (2). Previous studies have suggested that the pathways that control stimulus-responsive activation of the NF-κB dimers are highly interconnected (3). Not only were the canonical IKK2 and noncanonical IKK1 pathways both shown to activate NF-κB DNA binding activity in the nucleus, but these pathways also significantly cross talk with each other within the cellular milieu. Hence, we further attempted to map the signaling axis that mediates NF-κB activation upon JEV infection. To this end, nuclear extracts were prepared from wild-type MEFs at different time intervals after JEV infection and NF-κB activation was analyzed by EMSA using NF-κB-specific and mutant DNA oligomers. As shown in Fig. 1A, JEV infection induced the nuclear translocation of NF-κB in wild-type MEFs (lanes 1 to 4). As expected, there was no DNA binding with the mutant oligomer, confirming the specificity of the *in vitro* DNA binding assay. It has been reported that TNF-induced NF-κB activation is completely abrogated in MEFs deficient in both IKK1 and IKK2 subunits (24). To address the role of the IκB kinase (IKK) complex in JEV-infected cells, we first infected IKK1$^{-/-}$ IKK2$^{-/-}$ (IKK-deficient) MEFs and analyzed the NF-κB activation by EMSA. As shown in Fig. 1A, JEV-induced nuclear translocation of NF-κB was completely abolished in IKK-deficient cells (lanes 9 to 12), indicating the involvement of the IKK subunits. RelA$^{-/-}$ cRel$^{-/-}$ p50$^{-/-}$ (NF-κB-deficient) MEFs that are devoid of canonical NF-κB subunits were shown to completely lack the NF-κB activation during both canonical TNF receptor (TNFR) and noncanonical LTβR signaling (5). The complete absence of DNA binding in NF-κB-deficient MEFs upon JEV infection (lanes 13 to 16) was consistent with this previous finding and indicates a possible dominant role of the canonical dimers in the cellular response to JEV infection. Nevertheless, intracellular staining

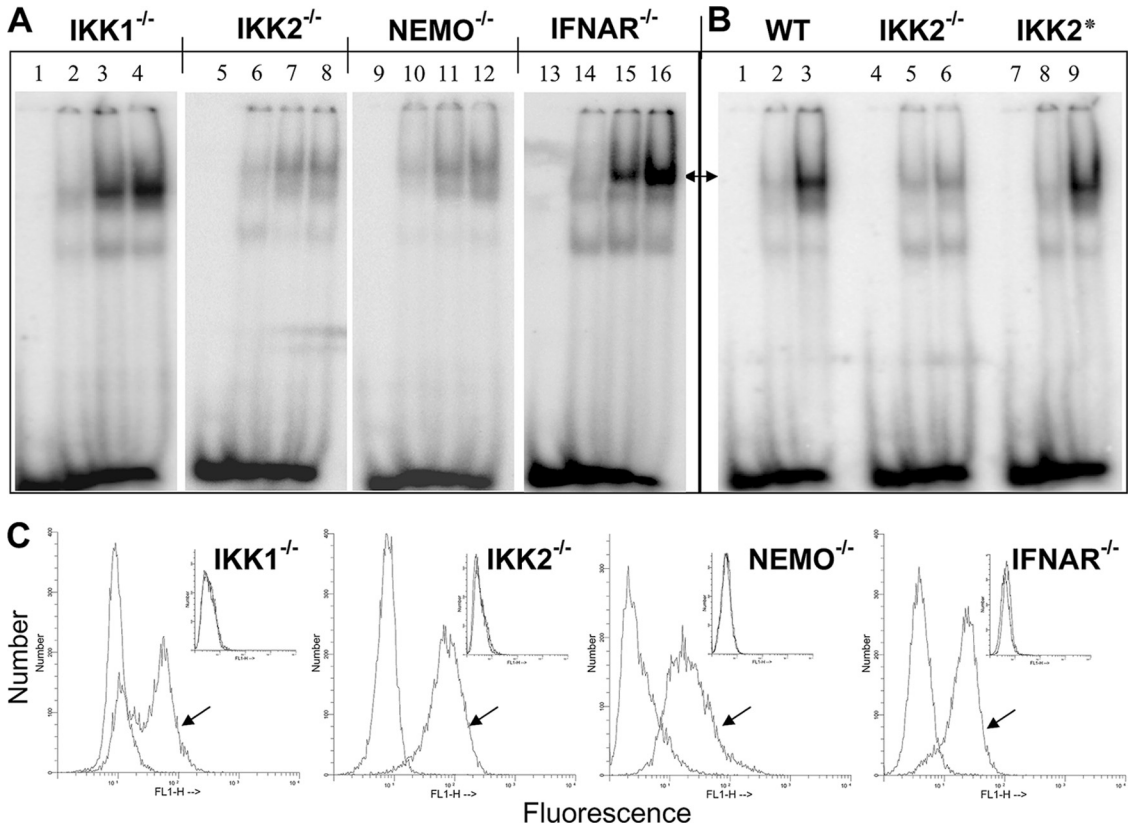


FIG. 2. Status of canonical and noncanonical pathways of NF-κB activation upon JEV infection. (A) EMSA was performed with uninfected and JEV-infected IKK1$^{-/-}$, IKK2$^{-/-}$, NEMO$^{-/-}$, and IFNAR$^{-/-}$ MEFs as indicated on top. Lanes 1, 5, 9, and 13 represent the oligomer alone; lanes 2, 6, 10, and 14 represent uninfected MEFs; lanes 3, 7, 11, and 15 represent cells infected for 10 h; and lanes 4, 8, 12, and 16 represent cells infected for 14 h. (B) EMSA was performed with wild-type (WT) and IKK2$^{-/-}$ MEFs and IKK2$^{-/-}$ MEFs that were reconstituted with the wild-type IKK2 transgene (IKK2*). Lanes 1, 4, and 7 represent oligomer alone, and lanes 2, 5, and 8 represent uninfected cells, while lanes 3, 6, and 9 represent infected cells. Arrows in panels A and B show the positions of the specific NF-κB complex. (C) As labeled, IKK1$^{-/-}$, IKK2$^{-/-}$, NEMO$^{-/-}$, and IFNAR$^{-/-}$ MEFs that were infected with JEV for 12 h were stained for the expression of intracellular JEV antigen. Arrows indicate staining with primary antiflavivirus group-specific MAb followed by fluorescein isothiocyanate (FITC) anti-mouse secondary antibody, while unmarked histograms indicate staining with secondary antibody alone. The two histograms overlap in the insets, which represent staining of uninfected cells.

for viral antigen of infected WT, IKK-deficient, and NF-κB-deficient MEFs at 12 h p.i. showed that all three cell types were infected (Fig. 1B), similarly indicating that the effects observed were not due to defective JEV infection.

**Delineating the JEV-induced NF-κB activation pathway.** Given that both IKK1 and IKK2 are capable of activating NF-κB, albeit through distinct mechanisms (4), we sought to examine the role of these individual IKK subunits in JEV-induced NF-κB activation. To this end, we infected wild-type, IKK1$^{-/-}$, or IKK2$^{-/-}$ MEFs and examined JEV-induced NF-κB activation at different time intervals after infection by EMSA (Fig. 2A). JEV-induced nuclear translocation of the NF-κB dimers was intact in IKK1$^{-/-}$ MEFs (Fig. 2A, lanes 1 to 4) but was severely attenuated in IKK2$^{-/-}$ MEFs (lanes 5 to 8) even at late time points. Furthermore, MEFs devoid of NEMO, an essential component of the canonical IKK2-containing kinase complex, also lack JEV-induced NF-κB activity (lanes 9 to 12).

To further validate the idea that the abrogated NF-κB activity in IKK2$^{-/-}$ MEFs was indeed due to the absence of IKK2 function, we utilized IKK2$^{-/-}$ cells that were reconstituted with a retrovirus expressing the wild-type IKK2 transgene (5). NF-κB activation was completely restored in this reconstituted cell line, further confirming a critical role of IKK2 in the induction of NF-κB during JEV infection (Fig. 2B, top, compare lane 6 and lane 9). Therefore, our results indicate that the canonical IKK2 pathway that transduces inflammatory signals from TNFR is also important for NF-κB activation during JEV infection, whereas the noncanonical IKK1 pathway is dispensable.

As NF-κB was shown to be activated by type I IFNs (11) and JEV is known to induce type I IFNs, we examined the role of type I IFN-mediated autocrine feedback in JEV-induced NF-κB activation. To this end, EMSA was performed utilizing nuclear extracts derived from IFNAR$^{-/-}$ MEFs infected with JEV, and the results show that NF-κB was indeed activated in these cells (Fig. 2A, lanes 13 to 16). These analyses suggest that JEV-induced NF-κB activation is independent of type 1 IFN signaling and depends on the canonical IKK2 activity. Alternatively, two functioning components, a type I IFN-dependent pathway and a type I IFN-independent pathway, may be involved in NF-κB activation and JEV may utilize the latter one in MEFs.

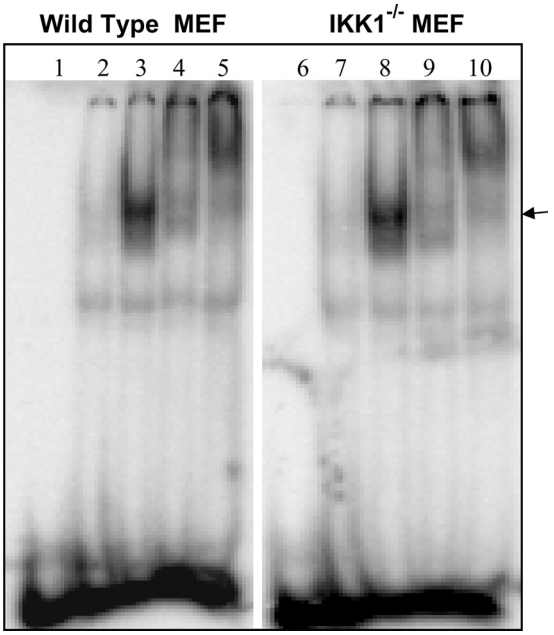


FIG. 3. JEV-activated NF-κB is composed of p50 and p65. EMSA and supershift assays were performed with nuclear extracts from wild-type and IKK1$^{-/-}$ MEFs as labeled on top. Lanes 1 and 6, oligomer alone; lanes 2 and 7, uninfected cells; lanes 3 and 8, infected cells obtained at 14 h p.i.; lanes 4 and 9, infected cells obtained at 14 h p.i. along with anti-RelA specific antibodies; lanes 5 and 10, infected cells obtained at 14 h p.i. along with anti-p50 specific antibodies. The arrow indicates the NF-κB–DNA binary complex that is supershifted upon addition of antibodies.

Intracellular staining for viral antigen of infected IKK1$^{-/-}$, IKK2$^{-/-}$, NEMO$^{-/-}$, and IFNAR$^{-/-}$ MEFs at 12 h p.i. revealed that all three cell types supported infection similarly (Fig. 2C), showing that the effects observed with IKK2$^{-/-}$ and NEMO$^{-/-}$ MEFs were not due to lack of efficient JEV infection.

Finally, we utilized nuclear extracts derived from wild-type MEFs infected with JEV in a supershift assay to determine the composition of the NF-κB dimers induced upon virus infection. As shown in Fig. 3, the NF-κB DNA binding complex induced upon JEV infection in wild-type (lanes 1 to 5) or IKK1$^{-/-}$ MEFs (lanes 6 to 10) was completely supershifted by RelA as well as p50-specific antibodies, indicating that the NF-κB/RelA:p50 dimer constitutes the major JEV-induced DNA binding dimer. Since JEV is neurotropic in nature, primary mouse brain astrocytes were also examined, and the results showed that the JEV-induced NF-κB activity was similarly composed of RelA and p50 dimers (data not shown).

**JEV-mediated induction of classical MHC-I gene (*H-2K$^b$* and *H-2D$^b$*) expression is not dependent directly on NF-κB.** It has been reported that WNV-induced expression of classical MHC-I molecules occurs by both NF-κB-dependent and -independent mechanisms (8). To determine the role of NF-κB in the induction of classical MHC-I molecules during JEV infection, we infected WT, IKK1$^{-/-}$, IKK2$^{-/-}$, NEMO$^{-/-}$, IKK1$^{-/-}$ IKK2$^{-/-}$, and RelA$^{-/-}$ cRel$^{-/-}$ p50$^{-/-}$ MEFs and analyzed the expression of classical MHC-I genes by semiquantitative and real-time RT-PCR analysis (Fig. 4 and Table 1).

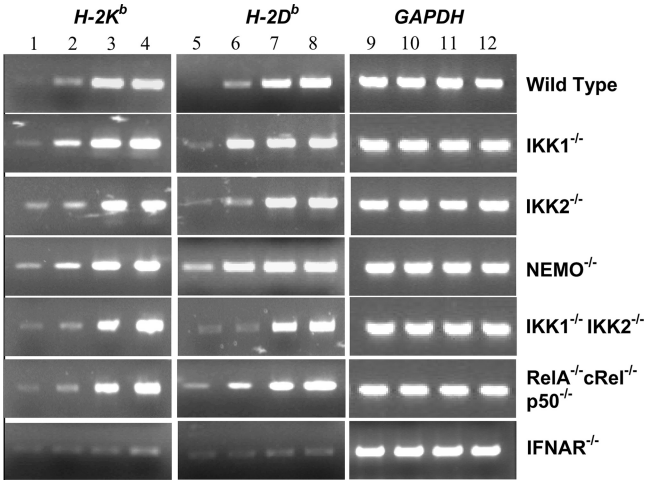


FIG. 4. RT-PCR analysis of classical MHC-I gene (*H-2K$^b$* and *H-2D$^b$*) expression in infected cells. RT-PCR analysis was carried out for 30 cycles with uninfected and JEV-infected wild-type, IKK1$^{-/-}$, IKK2$^{-/-}$, NEMO$^{-/-}$, IKK1$^{-/-}$ IKK2$^{-/-}$, RelA$^{-/-}$ cRel$^{-/-}$ p50$^{-/-}$, and IFNAR$^{-/-}$ MEFs as indicated. Lanes 1, 5, and 9 represent cells that were mock infected for 36 h. Lanes 2, 6, and 10 represent results obtained at 12 h after infection. Lanes 3, 7, and 11 represent cells obtained at 24 h p.i., while lanes 4, 8, and 12 represent cells at 36 h after infection.

Our studies clearly show that the fold induction of classical MHC-1 mRNAs upon JEV infection was not only intact in IKK1$^{-/-}$ MEFs but also relatively unaffected in IKK2$^{-/-}$, NEMO$^{-/-}$, IKK1$^{-/-}$ IKK2$^{-/-}$, and RelA$^{-/-}$ cRel$^{-/-}$ p50$^{-/-}$ MEFs that are defective in NF-κB activation (Table 1). Both *H-2K* and *H-2D* alleles were induced at 24 h (Fig. 4, lanes 3 and 7) and 36 h (lanes 4 and 8) p.i. in wild-type cells as well as in all five mutant cell lines. Since the NF-κB-independent mechanism of MHC-I induction utilized by WNV is mediated by type I IFNs (8), we analyzed IFNAR$^{-/-}$ MEFs, and our results clearly document that JEV-induced expression of classical MHC-I (*H-2K$^b$* and *D$^b$*) genes was significantly reduced in IFNAR$^{-/-}$ MEFs (Fig. 4 and Table 1). Therefore, our analyses suggest that classical MHC-I gene expression upon JEV infection is not directly dependent on NF-κB but depends largely on type I IFN signaling.

TABLE 1. Quantitative real-time RT-PCR analysis of MHC-I and type I IFN gene expression

| MEF type | Fold change (×10)[a,b,c] | | | |
|---|---|---|---|---|
| | *H-2K$^b$* | *H-2D$^b$* | *IFN*-α | *IFN*-β |
| WT | 16.2 ± 1.7 | 15.7 ± 0.7 | 191.0 ± 36.7 | 545.8 ± 35.6 |
| IKK1$^{-/-}$ | 16.2 ± 2.3 | 13.5 ± 1.5 | 187.9 ± 34.0 | 525.5 ± 14.4 |
| IKK2$^{-/-}$ | 13.0 ± 2.3 | 14.3 ± 1.7 | 50.2 ± 8.8 | 81.7 ± 9.1 |
| IKK2*[d] | ND[e] | ND | 128.8 ± 8.6 | 422.9 ± 40.0 |
| NEMO$^{-/-}$ | 16.4 ± 2.8 | 14.7 ± 2.9 | 38.3 ± 5.0 | 75.2 ± 11.3 |
| IKK1$^{-/-}$ IKK2$^{-/-}$ | 14.4 ± 3.0 | 13.5 ± 0.5 | 47.9 ± 7.9 | 80.5 ± 10.1 |
| RelA$^{-/-}$ cRel$^{-/-}$ p50$^{-/-}$ | 17.5 ± 0.8 | 16.0 ± 1.3 | 44.3 ± 11.1 | 81.5 ± 17.6 |
| IFNAR$^{-/-}$ | 0.7 ± 0.0 | 0.4 ± 0.1 | 0.6 ± 0.2 | 45.9 ± 7.1 |

[a] Fold change is represented as mean ± standard deviation of three independent PCR analyses of the same cDNA sample used for Fig. 4 and 5.
[b] H-2 gene expression was analyzed at 36 h p.i.
[c] IFN gene expression was analyzed at 24 h p.i.
[d] IKK2$^{-/-}$ cells reconstituted with wild-type IKK2.
[e] ND, not done.

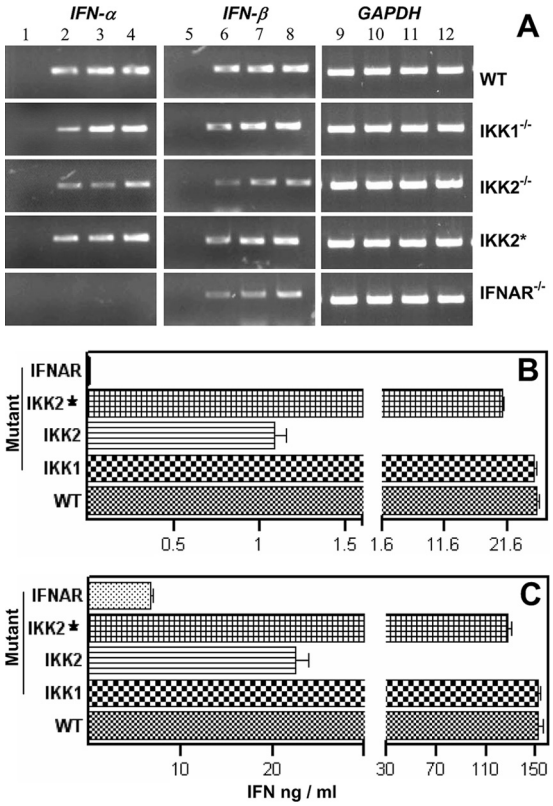


FIG. 5. Quantification of type I IFN production by RT-PCR analysis and ELISA. (A) As indicated on top, RT-PCR analysis of *IFN*-α, *IFN*-β, and *GAPDH* expression was performed for 27 cycles using JEV-infected wild-type (WT), IKK1$^{-/-}$, and IKK2$^{-/-}$ MEFs; IKK2$^{-/-}$ cells that were reconstituted with the wild-type IKK2 transgene (IKK2*); and IFNAR$^{-/-}$ MEFs. Lanes 1, 5, and 9 represent cells that were mock infected for 36 h; lanes 2, 6, and 10 represent cells that were infected for 12 h; lanes 3, 7, and 11 represent cells at 24 p.i.; and lanes 4, 8, and 12 represent cells obtained at 36 h after infection. (B and C) Quantification of IFN-α and IFN-β in the supernatants of JEV-infected MEFs. As indicated on the left, wild-type (WT), IKK1$^{-/-}$, and IKK2$^{-/-}$ MEFs; IKK2$^{-/-}$ cells that were reconstituted with the wild-type IKK2 transgene (IKK2*); and IFNAR$^{-/-}$ MEFs were infected for 36 h, and the levels of IFN-α (B) and IFN-β (C) in culture supernatants were analyzed by ELISA. Data represent the mean levels of IFN (ng/ml) produced from $2 \times 10^6$ cells ± standard errors of the means of triplicate assays in a total volume of 2.5 ml.

**NF-κB is involved in the production of type I IFNs in MEFs upon JEV infection.** Given that classical MHC-I gene expression relies largely on type I IFN and not on NF-κB signaling, we asked if the production of IFN-α and IFN-β is intact in cells defective in NF-κB activation. As shown in Fig. 5A, our RT-PCR analysis revealed that JEV infection similarly induced the expression of *IFN*-α and *IFN*-β in wild-type and IKK1$^{-/-}$ MEFs. However, the fold induction in the expression of type I IFN genes was reduced but not completely abolished in IKK2$^{-/-}$ MEFs (Table 1) as well as in NEMO$^{-/-}$, IKK1$^{-/-}$ IKK2$^{-/-}$, and RelA$^{-/-}$ cRel$^{-/-}$ p50$^{-/-}$ MEFs that lack JEV-induced NF-κB activation (see Fig. S2A in the supplemental material). It was also observed that the fold decrease in the expression of IFN-α was greater than that of IFN-β in the above-mentioned mutants and that its expression decreased further but was not abolished in IFNAR$^{-/-}$ MEFs (Table 1).

Time course ELISA analysis (see Fig. S2B and S2C in the supplemental material) using virus-infected wild-type MEFs showed that maximum amounts of type I IFNs were present in the culture supernatants at 36 h after infection. Hence, type I IFN production levels were compared at 36 h p.i. using wild-type and mutant MEFs. As shown in Fig. 5B and 5C, there was a significant reduction in the levels of both IFN-α and IFN-β in the supernatants of JEV-infected IKK2$^{-/-}$ but not in IKK1$^{-/-}$ MEFs. While IFN-β levels were reduced further in IFNAR$^{-/-}$ MEFs, IFN-α levels were negligible. Reduced type I IFN levels were also observed in NEMO$^{-/-}$, IKK1$^{-/-}$ IKK2$^{-/-}$, and RelA$^{-/-}$ cRel$^{-/-}$ p50$^{-/-}$ MEFs (see Fig. S2B and S2C). These observations further suggested that type I IFN induction by JEV utilizes both NF-κB-dependent and NF-κB-independent mechanisms and that the NF-κB-independent activation of type I IFNs may be sufficient to drive classical MHC-I gene expression.

To further validate the idea that the reduced production of type I IFNs in IKK2$^{-/-}$ cells was indeed due to the absence of IKK2 function, we utilized IKK2$^{-/-}$ cells that were reconstituted with a retrovirus expressing the wild-type IKK2 transgene. As shown in Fig. 5 and Table 1, IKK2 reconstitution (IKK2*) clearly restored the ability of IKK2$^{-/-}$ cells not only to induce significant IFN-α and IFN-β gene expression (Fig. 5A) but also to produce IFN-α and IFN-β upon JEV infection (Fig. 5B and 5C).

**JEV-induced surface expression of MHC-I is reduced in MEFs deficient in type I interferon but not in NF-κB signaling.** Infected wild-type and mutant MEFs were analyzed by FACS in order to address the role of endogenously produced type I IFNs in JEV-mediated induction of H-2K$^b$ and H-2D$^b$ classical MHC-I molecules on the cell surface. As shown in Fig. 6A and B, cell surface expression of MHC-I was intact in all mutant cells that are devoid of NF-κB function despite reduced type I IFN production in the culture supernatants. However, JEV-induced cell surface expression of MHC-I was completely abolished in IFNAR$^{-/-}$ MEFs (Fig. 6B). To address if the low level of IFNs produced through an NF-κB-independent mechanism was sufficient for classical MHC-I expression, control wild-type MEFs were cultured using various amounts of exogenously added type I IFNs. As shown in Fig. 6C, addition of as low a concentration as 1 ng/ml of either IFN-α (middle) or IFN-β (right) significantly induced cell surface expression of MHC-I, suggesting that the low levels of type I IFNs produced by mutant MEFs were sufficient to induce cell surface MHC-I expression that is comparable to JEV infection (left). These observations also indicated that type I IFNs, not NF-κB, play a major role in the induction of MHC-I molecules upon JEV infection.

We have earlier shown that this neurotropic virus induces the cell surface expression of classical MHC-I molecules not only in primary mouse brain astrocytes and wild-type MEFs but also in L929 and 3T3 mouse fibroblasts and murine H-6 hepatoma cells (2). In addition, flaviviruses are reported to infect many cell types (21). Although all the above studies utilized MEFs due to the availability of appropriate mutant MEFs, it was observed that the ability of JEV to activate NF-κB was also considerably reduced in H-6 hepatoma cells relative to WT MEFs (see Fig. S3A in the supplemental material). This effect was examined further since H-6 has been

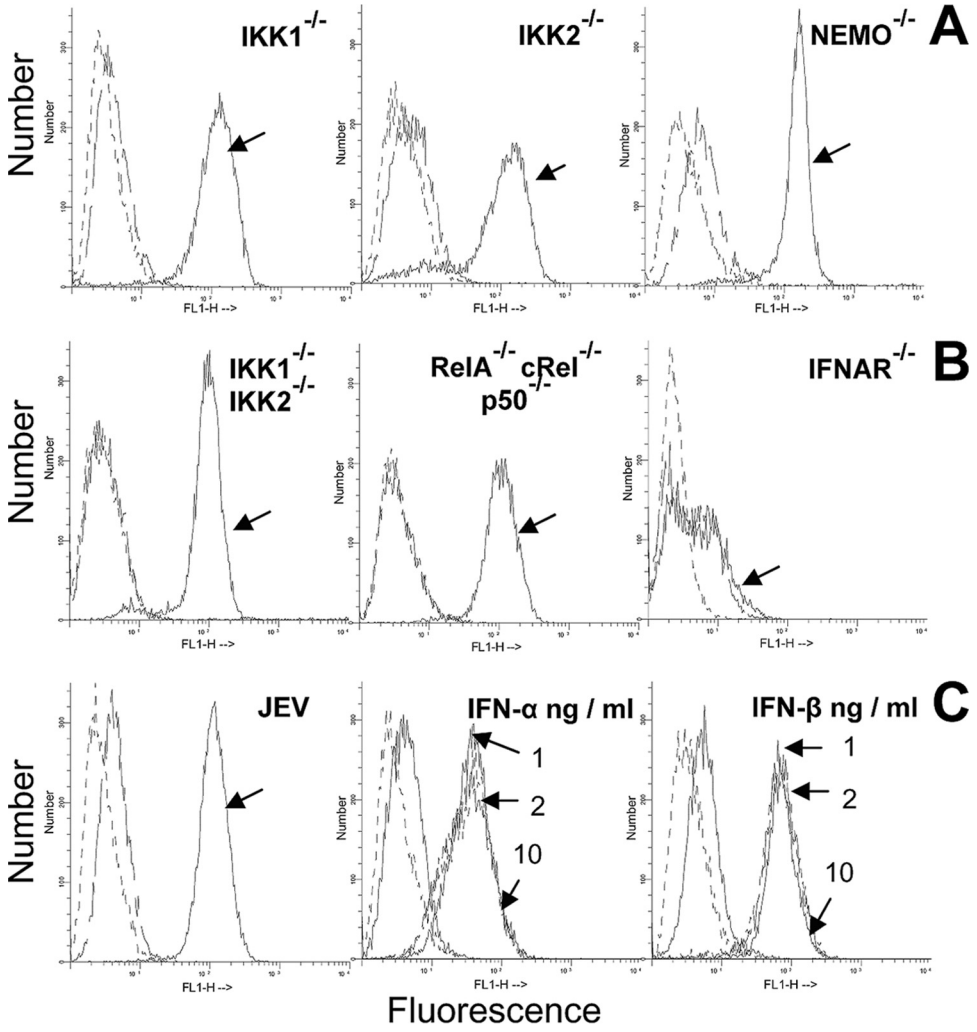


FIG. 6. Cell surface expression of classical MHC-I (H-$2^b$) antigens. (A) Flow cytometric analysis of H-$2^b$ expression on control and JEV-infected IKK1$^{-/-}$, IKK2$^{-/-}$, and NEMO$^{-/-}$ MEFs at 36 h after infection. (B) H-$2^b$ expression on control and IKK1$^{-/-}$ IKK2$^{-/-}$, RelA$^{-/-}$ cRel$^{-/-}$ p50$^{-/-}$, and IFNAR$^{-/-}$ MEFs that were infected with JEV for 36 h. (C) H-$2^b$ expression on uninfected and infected wild-type cells at 36 h p.i. is shown at left. Staining with primary (anti-H-$2^b$ specific MAb) and fluorescein isothiocyanate (FITC) anti-mouse secondary antibody is indicated by arrows for infected cells and by unmarked broken lines for uninfected cells, while dashed lines indicate staining with secondary antibody alone. Figures in the middle (IFN-α) and right (IFN-β) of the panel represent H-$2^b$ expression on wild-type MEFs treated for 36 h with 1, 2, and 10 ng/ml of either IFN-α or IFN-β, respectively, as indicated by arrows. The same standard IFNs obtained for ELISA measurements were used. In all histograms, dashed lines represent staining with FITC-conjugated secondary antibody alone, while H-$2^b$ expression is indicated by unmarked lines in untreated cells and arrow marks in treated/uninfected cells.

utilized as a model system to study the role of IFNs in the induction of MHC-I as well as molecules involved in antigen presentation (33). The ability of H-6 to upregulate cell surface expression of MHC-I upon JEV infection remained unaffected despite the concomitant decrease in type I IFN production, suggesting that the decreased ability of JEV to induce type I IFN production in the absence of NF-κB activation also occurred in H-6 hepatoma cells.

## DISCUSSION

NF-κB controls the expression of genes involved in immune responses, apoptosis, and the cell cycle (6, 18, 38). It has been shown to play a major role in flavivirus-mediated induction of MHC antigens (8, 9, 21), and viral modulation of the NF-κB pathway is well known (6, 17, 41). In addition to NF-κB activation, MHC-I induction by flavivirus has also been reported to be due to increased peptide transport into the lumen of the endoplasmic reticulum (29). Our earlier study with mouse brain astrocytes showed that JEV infection results in the induction of the nonclassical MHC-I H-2T23, H-2Q4, and H-2T10 genes in addition to MHC-I, Tap1, Tap2, Tapasin, Lmp2, Lmp7, and Lmp10 but not CD80, CD86, and MHC-II genes (2). Since NF-κB can be activated by two distinct pathways—canonical and noncanonical—we have used mutant MEFs devoid of different signaling components to examine their respective roles in MHC-I induction by JEV. The canonical pathway functions to maintain the survival of immune cells during bacterial and inflammatory stimulation. In contrast, the noncanonical pathway is associated with the development of

lymphoid organs that ensure the mounting of an effective immune response (3, 6). Our finding that JEV infection activates the canonical NF-κB pathway is clearly supported by data involving EMSA and gene transcription as well as cell surface expression analyses. It is possible that this strategy may help to delay cellular apoptosis in cells infected with a cytopathic virus such as JEV.

To analyze the role of interferon and NF-κB signaling during JEV infection, we used different knockout MEFs, which are defective either in NF-κB or in interferon signaling. The abilities of these mutant cell lines to support comparable levels of infection by JEV were ascertained by measuring the presence of intracellular viral antigen (Fig. 1 and 2) as well as the production of virus in cell culture supernatants. Virus titers obtained 36 h after infection were comparable in all the cells used in this study except for IFNAR$^{-/-}$ MEFs, where the titers were 3- to 4-fold higher. However, infection of IFNAR$^{-/-}$ MEFs at lower MOIs of 0.5 and 0.1 did not result in either MHC-I induction or type I IFN production (data not shown), and we have reported earlier that JEV was able to induce the expression of T10, a nonclassical MHC-I gene, in IFNAR$^{-/-}$ cells (2) when infected under similar conditions. Hence, we believe that the consequences of higher virus replication would not explain the observed lack of JEV-induced MHC expression in these mutants. Nuclear translocation of NF-κB was robustly induced in JEV-infected wild-type or IKK1$^{-/-}$ MEFs but decreased significantly in IKK2$^{-/-}$ and NEMO$^{-/-}$ MEFs, whereas it was completely abolished in IKK1$^{-/-}$ IKK2$^{-/-}$ (IKK-deficient) MEFs. These studies that use MEFs deficient in different subunits of IκB kinase (IKK) complex were further substantiated by using MEFs deficient in NF-κB proteins—p50, RelA, and cRel (NF-κB deficient)—and our results show that NF-κB activation was also completely abolished in MEFs deficient in canonical NF-κB proteins.

The manner in which these pathways are activated by JEV and the involvement of JEV proteins in the process of NF-κB activation are presently unknown. It has been shown that Toll-like receptor 3 (TLR3) is involved in the entry of the related flavivirus WNV into cells (40), and since TLRs are capable of activating NF-κB, TLR3 could be involved in NF-κB activation upon JEV infection. Other candidates include RIG-I (RNA helicase) or PKR, each of which is able to recognize double-stranded RNA (dsRNA), which finally leads to NF-κB activation (20, 42). The functional significance of JEV-induced NF-κB activation in the induction of MHC-I molecules was examined, since other flaviviruses have been shown to induce MHC-I in an NF-κB-dependent manner (8, 22). However, it was observed that MHC-I induction by JEV remained intact despite the absence of NF-κB activation. Along with the observation that MHC-I was not inducible by JEV in IFNAR$^{-/-}$ cells, this suggested that MHC-I induction in JEV-infected MEFs was largely type I IFN dependent and NF-κB independent. These observations suggest that JEV differs from WNV, a related flavivirus, not only with regard to its ability to induce MHC-I in an NF-κB-independent manner but also with regard to its inability to induce MHC-II, in contrast to WNV (21).

Our results also suggest a role for NF-κB in the induction of type I IFNs during JEV infection. JEV-induced type I IFN production was significantly reduced in cells that were deficient in NF-κB activation. Our observation is explained by the previous findings that IFN-β is known to be regulated by NF-κB and that production of IFN-α requires IFN-β and is completely abolished in MEFs deficient in IFN-β production (12, 30). Hence, the reduced levels of IFN-α in cells defective in NF-κB function could be due to decreased IFN-β production. Intact cell surface MHC-I expression despite decreased IFN production may be due to the possibility that the decreased levels of IFN produced in these NF-κB-deficient cells upon virus infection were sufficient to bring about induction of MHC-I (Fig. 6C). The lack of induction of cell surface MHC-I expression in IFNAR$^{-/-}$ cells despite the presence of type I IFNs in the culture supernatant, although at lower concentrations, is explained by the lack of functional receptor. These cells also lack MHC-I induction upon exogenous addition of type I IFNs (data not shown).

JEV is known to block IFN-stimulated Jak-Stat signaling by preventing Tyk2 and Stat phosphorylation (26, 27). However, although we observed a modest decrease in type I IFNs (1) at 48 h p.i. (see Fig. S2B and C in the supplemental material), no inhibition of MHC-I expression was observed either in primary astrocytes (2) or in wild-type and mutant MEFs (this study). TNF is known to induce MHC-I expression (10), and TNF levels increase in JEV patients (34) as well as in WNV-infected MEFs (9). IKK2$^{-/-}$ MEFs that lack TNF-induced NF-κB activation reveal intact MHC-I expression upon JEV infection, although their failure to respond significantly to exogenously added TNF compared to WT cells was verified (see Fig. S1A, lanes 6 and 7, and Fig. S1B, lanes 5 and 6). Hence, the contribution of TNF to MHC-I expression in mutant or wild-type cells is unlikely. WNV-induced MHC-I has also been reported to be TNF independent (9).

Hence, residual type I IFNs produced by NF-κB-independent mechanisms possibly mediated by IFN regulatory factor 3 (IRF3) may also play a role in inducing the expression of classical MHC-I molecules during JEV infection. Additional activation pathways for type I IFNs involving TLRs and RIG-I/MDA-5-mediated activation of IRF3 and IRF7 have also been reported for JEV, WNV, and dengue virus (7). In summary, to our knowledge, this is the first report in which the status of canonical and noncanonical pathways of NF-κB activation as well as the relatively NF-κB-independent nature of classical MHC-I induction has been shown during JEV infection. However, the possibility that different cell types may engage a different mechanism to induce MHC-I upon infection with this neurotropic virus cannot be unambiguously ruled out.

## ACKNOWLEDGMENTS

This work was supported by a grant from CSIR, Government of India, and partly by DAE, Government of India. All flow cytometry studies were performed using the BD FACScan instrument at the Central Instrument Facility, which received funding from the Department of Biotechnology, Government of India.

Cytometry operations were performed by Omana Joy and M. Vamsi. We thank Tejaswini Kulkarni, M. V. Sreedevi, and Aruna Sreenivasan for assistance at various stages of the project. We also thank Alexander Hoffmann, UCSD, for his valuable suggestions and critical discussions.

## REFERENCES

1. **Abraham, S., and R. Manjunath.** 2006. Induction of classical and nonclassical MHC-I on mouse brain astrocytes by Japanese encephalitis virus. Virus Res. **119:**216–220.
2. **Abraham, S., K. Yaddanapudi, S. Thomas, A. Damodaran, B. Ramireddy,**

**and R. Manjunath.** 2008. Nonclassical MHC-I and Japanese encephalitis virus infection: induction of H-2Q4, H-2T23 and H-2T10. Virus Res. **133:** 239–249.
3. **Basak, S., and A. Hoffmann.** 2008. Crosstalk via the NF-kappaB signaling system. Cytokine Growth Factor Rev. **19:**187–197.
4. **Basak, S., H. Kim, J. D. Kearns, V. Tergaonkar, E. O'Dea, S. L. Werner, C. A. Benedict, C. F. Ware, G. Ghosh, I. M. Verma, and A. Hoffmann.** 2007. A fourth IKappaB protein within the NF-kappaB signaling module. Cell **128:**369–381.
5. **Basak, S., V. F. Shih, and A. Hoffmann.** 2008. Generation and activation of multiple dimeric transcription factors within the NF-kappaB signaling system. Mol. Cell. Biol. **28:**3139–3150.
6. **Bonizzi, G., and M. Karin.** 2004. The two NF-kappaB activation pathways and their role in innate and adaptive immunity. Trends Immunol. **25:**280–288.
7. **Chang, T. H., C. L. Liao, and Y. L. Lin.** 2006. Flavivirus induces interferon-beta gene expression through a pathway involving RIG-I-dependent IRF-3 and PI3K-dependent NF-kappaB activation. Microbes Infect. **8:**157–171.
8. **Cheng, Y., N. J. King, and A. M. Kesson.** 2004. Major histocompatibility complex class I (MHC-I) induction by West Nile virus: involvement of 2 signaling pathways in MHC-I up-regulation. J. Infect. Dis. **189:**658–668.
9. **Cheng, Y., N. J. King, and A. M. Kesson.** 2004. The role of tumor necrosis factor in modulating responses of murine embryo fibroblasts by flavivirus, West Nile. Virology **329:**361–370.
10. **Drew, P. D., G. Franzoso, K. G. Becker, V. Bours, L. M. Carlson, U. Siebenlist, and K. Ozato.** 1995. NF kappa B and interferon regulatory factor 1 physically interact and synergistically induce major histocompatibility class I gene expression. J. Interferon Cytokine Res. **15:**1037–1045.
11. **Du, Z., L. Wei, A. Murti, S. R. Pfeffer, M. Fan, C. H. Yang, and L. M. Pfeffer.** 2007. Non-conventional signal transduction by type-I interferons: the NK-κB pathway. J. Cell. Biochem. **102:**1087–1094.
12. **Erlandsson, L., R. Blumenthal, M. L. Eloranta, H. Engel, G. Alm, S. Weiss, and T. Leanderson.** 1998. Interferon-beta is required for interferon-alpha production in mouse fibroblasts. Curr. Biol. **8:**223–226.
13. **Ghosh, S., and M. Karin.** 2002. Missing pieces in the NF-kappaB puzzle. Cell **109:**S81–S96.
14. **Haller, O., G. Kochs, and F. Weber.** 2006. The interferon response circuit: induction and suppression by pathogenic viruses. Virology **344:**119–130.
15. **Halstead, S. B., and J. Jacobson.** 2003. Japanese encephalitis. Adv. Virus Res. **61:**103–138.
16. **Heinz, F. X., and S. L. Allison.** 2000. Structures and mechanisms in flavivirus fusion. Adv. Virus Res. **55:**231–269.
17. **Hiscott, J., T. L. Nguyen, M. Arguello, P. Nakhaei, and S. Paz.** 2006. Manipulation of the nuclear factor-kappaB pathway and the innate immune response by viruses. Oncogene **25:**6844–6867.
18. **Hoffmann, A., and D. Baltimore.** 2006. Circuitry of nuclear factor kappaB signaling. Immunol. Rev. **210:**171–186.
19. **Honda, K., H. Yanai, A. Takaoka, and T. Taniguchi.** 2005. Regulation of the type I IFN induction: a current view. Int. Immunol. **17:**1367–1378.
20. **Kato, H., S. Sato, M. Yoneyama, M. Yamamoto, S. Uematsu, K. Matsui, T. Tsujimura, K. Takeda, T. Fujita, O. Takeuchi, and S. Akira.** 2005. Cell type-specific involvement of RIG-I in antiviral response. Immunity **23:**19–28.
21. **Kesson, A. M., Y. Cheng, and N. J. King.** 2002. Regulation of immune recognition molecules by flavivirus, West Nile. Viral Immunol. **15:**273–283.
22. **Kesson, A. M., and N. J. King.** 2001. Transcriptional regulation of major histocompatibility complex class I by flavivirus West Nile is dependent on NF-kappaB activation. J. Infect. Dis. **184:**947–954.
23. **Kurane, I.** 2002. Immune responses to Japanese encephalitis virus. Curr. Top. Microbiol. Immunol. **267:**91–103.
24. **Li, Q., G. Estepa, S. Memet, A. Israel, and I. M. Verma.** 2000. Complete lack of NF-kappaB activity in IKK1 and IKK2 double-deficient mice: additional defect in neurulation. Genes Dev. **14:**1729–1733.
25. **Li, Q., and I. M. Verma.** 2002. NF-kappaB regulation in the immune system. Nat. Rev. Immunol. **2:**725–734.
26. **Lin, C. W., C. W. Cheng, T. C. Yang, S. W. Li, M. H. Cheng, L. Wan, Y. J. Lin, C. H. Lai, W. Y. Lin, and M. C. Kao.** 2008. Interferon antagonist function of Japanese encephalitis virus NS4A and its interaction with DEAD-box RNA helicase DDX42. Virus Res. **137:**49–55.
27. **Lin, R. J., C. L. Liao, E. Lin, and Y. L. Lin.** 2004. Blocking of the alpha interferon-induced Jak-Stat signaling pathway by Japanese encephalitis virus infection. J. Virol. **78:**9285–9294.
28. **Lindenbach, B. D., and C. M. Rice.** 2003. Molecular biology of flaviviruses. Adv. Virus Res. **59:**23–61.
29. **Lobigs, M., A. Mullbacher, and M. Regner.** 2003. MHC class I up-regulation by flaviviruses: immune interaction with unknown advantage to host or pathogen. Immunol. Cell Biol. **81:**217–223.
30. **MacDonald, N. J., D. Kuhl, D. Maguire, D. Naf, P. Gallant, A. Goswamy, H. Hug, H. Bueler, M. Chaturvedi, J. de la Fuente, H. Ruffner, F. Meyer, and C. Weissmann.** 1990. Different pathways mediate virus inducibility of the human IFN-alpha 1 and IFN-beta genes. Cell **60:**767–779.
31. **Muller, J. R., and U. Siebenlist.** 2003. Lymphotoxin beta receptor induces sequential activation of distinct NF-kappa B factors via separate signaling pathways. J. Biol. Chem. **278:**12006–12012.
32. **Platanias, L. C.** 2005. Mechanisms of type-I- and type-II-interferon-mediated signalling. Nat. Rev. Immunol. **5:**375–386.
33. **Prasanna, S. J., and D. Nandi.** 2004. The MHC-encoded class I molecule, H-2K$^k$ demonstrates distinct requirements of assembly factors for cell surface expression: role of Tap, Tapasin and $\beta_2$-microglobulin. Mol. Immunol. **41:**1029–1045.
34. **Ravi, V., S. Parida, A. Desai, A. Chandramuki, M. Gourie-Devi, and G. E. Grau.** 1997. Correlation of tumor necrosis factor levels in the serum and cerebrospinal fluid with clinical outcome in Japanese encephalitis patients. J. Med. Virol. **51:**132–136.
35. **Scheidereit, C.** 2006. IkappaB kinase complexes: gateways to NF-kappaB activation and transcription. Oncogene **25:**6685–6705.
36. **Senftleben, U., Y. Cao, G. Xiao, F. R. Greten, G. Krähn, G. Bonizzi, Y. Chen, Y. Hu, A. Fong, S. C. Sun, and M. Karin.** 2001. Activation by IKK alpha of a second, evolutionary conserved, NF-kappa B signaling pathway. Science **293:**1495–1499.
37. **Solomon, T.** 2003. Recent advances in Japanese encephalitis. J. Neurovirol. **9:**274–283.
38. **Tumang, J. R., A. Owyang, S. Andjelic, Z. Jin, R. R. Hardy, M. L. Liou, and H. C. Liou.** 1998. c-Rel is essential for B lymphocyte survival and cell cycle progression. Eur. J. Immunol. **28:**4299–4312.
39. **Vallabhapurapu, S., and M. Karin.** 2009. Regulation and function of NF-kappaB transcription factors in the immune system. Annu. Rev. Immunol. **27:**693–733.
40. **Wang, T., T. Town, L. Alexopoulou, J. F. Anderson, E. Fikrig, and R. A. Flavell.** 2004. Toll-like receptor 3 mediates West Nile virus entry into the brain causing lethal encephalitis. Nat. Med. **10:**1366–1373.
41. **You, L. R., C. M. Chen, and Y. H. Lee.** 1999. Hepatitis C virus core protein enhances NF-kappaB signal pathway triggering by lymphotoxin-beta receptor ligand and tumor necrosis factor alpha. J. Virol. **73:**1672–1681.
42. **Zamanian-Daryoush, M., T. H. Mogensen, J. A. DiDonato, and B. R. Williams.** 2000. NF-kappaB activation by double-stranded-RNA-activated protein kinase (PKR) is mediated through NF-kappaB-inducing kinase and IkappaB kinase. Mol. Cell. Biol. **20:**1278–1290.